

New Blue and Red Variable Stars in NGC 247

T.J. Davidge^{1,2,3}

Dominion Astrophysical Observatory,

Herzberg Astronomy & Astrophysics Research Center,

National Research Council of Canada, 5071 West Saanich Road,

Victoria, BC Canada V9E 2E7

tim.davidge@nrc.ca; tdavidge1450@gmail.com

ABSTRACT

Images recorded with the Gemini Multi-Object Spectrograph (GMOS) on Gemini South are combined with archival images from other facilities to search for variable stars in the southern portion of the nearby disk galaxy NGC 247. Fifteen new periodic and non-periodic variables are identified. These include three Cepheids with periods < 25 days, four semi-regular variables, one of which shows light variations similar to those of RCrB stars, five variables with intrinsic visible/red brightnesses and colors that are similar to those of luminous blue variables (LBVs), and three fainter blue variables, one of which may be a non-eclipsing close binary system. The S Doradus instability strip defines the upper envelope of a distinct sequence of objects on the $(i, g-i)$ color-magnitude diagram (CMD) of NGC 247. The frequency of variability with an amplitude ≥ 0.1 magnitude in the part of the CMD that contains LBVs over the seven month period when the GMOS images were recorded is ~ 0.2 . The light curve of the B[e] supergiant J004702.18–204739.9, which is among the brightest stars in NGC 247, is also examined. Low amplitude variations on day-to-day timescales are found, coupled with a systematic trend in mean brightness over a six month time interval.

¹Based on observations obtained at the Gemini Observatory, which is operated by the Association of Universities for Research in Astronomy, Inc., under a cooperative agreement with the NSF on behalf of the Gemini partnership: the National Science Foundation (United States), the National Research Council (Canada), CONICYT (Chile), Ministério da Ciência, Tecnologia e Inovação (Brazil) and Ministerio de Ciencia, Tecnología e Innovación Productiva (Argentina).

²This research has made use of the NASA/IPAC Infrared Science Archive, which is funded by the National Aeronautics and Space Administration and operated by the California Institute of Technology.

³This research has made use of the NASA/IPAC Extragalactic Database (NED), which is operated by the Jet Propulsion Laboratory, California Institute of Technology, under contract with the National Aeronautics and Space Administration.

1. INTRODUCTION

Variable stars have long been recognized as important probes of stars and stellar systems (e.g. Russell 1912a,b, Hubble 1925). Intrinsically luminous periodic variables such as Cepheids, eclipsing binaries (EBs), and long period variables are standard candles for distance measurements. The study of variable stars in galaxies that sample a range of metallicities also has the potential to yield constraints on stellar structure models. For example, the properties of massive EBs, such as the fraction that are in contact systems, may yield insights into mass loss rates from the component stars and the evolution of the close binary systems that play important roles in the chemical enrichment histories of galaxies (e.g. Sana et al. 2012; Howard et al. 2019). While EBs in the Magellanic Clouds are the prime targets for such studies (e.g. Davidge 1988; Almeida et al. 2015) given that their component stars have metallicities that are systematically different from those in the Galactic disk and are in the nearest extragalactic systems, studies of EBs in more distant galaxies will increase the sample size and have the potential to identify rare systems (e.g. Prieto et al. 2008). The study of luminous blue variables (LBVs) and related objects in galaxies that span a range of metallicities will provide insights into the processes that regulate the formation and evolution of the most massive stars, and provide constraints on their spectrophotometric properties. The environment of LBVs is of particular interest for interpreting the nature of these objects (e.g. Smith & Tombleson 2015; Humphreys et al. 2016).

NGC 247 is an SAB(s)d galaxy that is in one of the nearest external groups. While there are many late-type galaxies within a few Mpc of the Galaxy, NGC 247 is one of only a handful that have large-scale structural characteristics that hint at tidal interactions within the recent past. The HI disk is truncated (Carignan & Puche 1990), and there are asymmetries in the disk (e.g. Carignan 1985), including a lop-sided morphology due to a tidal arm (Davidge 2021). There is also evidence for an elevated SFR within the past Gyr (Davidge 2021; Kacharov et al. 2018), although the SFR at the present day is relatively low (Ferguson et al. 1996), with the peak brightness of the main sequence suggesting a marked decline in the past few Myr (Davidge 2006).

While we are not aware of published abundance measurements of HII regions in NGC 247, it has an M_K that is similar to that of M33 (Jarrett et al. 2003). The metallicities of young stars in these two galaxies should then be similar. The oxygen abundances of HII regions in M33 are similar to those in the LMC (e.g. Figure 4 of Toribio San Cipriano et al. 2017), and so the metallicity of NGC 247 is likely comparable to that of the LMC. There is also evidence that there is not a steep abundance gradient in the NGC 247 disk, as the colors of red supergiants (RSGs) throughout its disk suggest that the metallicity of these objects does not vary by more than ~ 0.1 dex over most of the young disk (Davidge 2006).

Thus, luminous variable stars found throughout the disk of NGC 247 should have similar metallicities.

The structural characteristics and stellar content of NGC 247 are also of interest as it is located within a few hundred kpc of the starburst galaxy NGC 253 (e.g. Karachentsev et al. 2003). Along with M82, NGC 253 is one of the nearest starburst galaxies, and so is an obvious target for understanding the origins and evolution of starburst activity. Unlike M82, an unambiguous trigger for starburst activity in NGC 253 has not yet been identified. An interaction with a large companion like NGC 247 is one possibility, and the timing of the onset of elevated SFRs in NGC 247 and NGC 253 more-or-less coincide (Davidge 2021), even though the SFR of NGC 247 has declined within the past few million years (Ferguson et al. 1996; Davidge 2006).

The variable star content of NGC 247 has not been extensively explored, and past studies have targeted only certain types of objects. The Aracauria project (Gieren et al. 2005) detected 23 Cepheids in NGC 247 that span a range of periods (Garcia-Varela et al. 2008). There are hints that the distribution of Cepheids throughout the galaxy may not be uniform, as only six Cepheids were found in the southern part of NGC 247, while Cepheids with periods < 30 days were found exclusively in the northern part of the disk. The distribution of Cepheids may then track the lop-sided morphology of the galaxy. As for other types of variable stars, Solovyeva et al. (2020) examined the spectrophotometric properties of two very luminous stars in the southern half of NGC 247, classifying one as a candidate LBV and the other as a B[e] supergiant.

In the current paper we present the results of a search for variable stars in the southern disk of NGC 247. The primary dataset consists of g' images recorded with the Gemini Multi-Object Spectrograph (GMOS) on Gemini South (GS) during a seven month period in 2008 and 2009. The identification of OB EBs was assigned a high priority, and the g' filter was selected to target stars with early spectral-types. The observing cadence was also set so that variability on timescales appropriate for such EBs (i.e. a few days to tens of days) was sampled. This sampling is also effective in the detection of other types of variables. The GMOS images are supplemented with observations from the Canada-France-Hawaii Telescope (CFHT) MegaCam and National Optical Astronomy Observatories (NOAO) DECam.

The datasets that are used in this paper and the processing that was performed on them are the subject of Section 2. The photometric measurements and the methodology for identifying objects with variable light measurements are discussed in Section 3. Light curves – phased according to periods when possible – are presented in Section 4, while the locations of the variables on color-magnitude diagrams (CMDs) and within NGC 247 are examined in Section 5. An investigation of variability among photometrically selected early-type stars

follows in Section 6. The paper closes in Section 7 with a brief discussion and summary of the results.

2. OBSERVATIONS & REDUCTION

2.1. GMOS Observations

NGC 247 was observed with GMOS on GS (Hook et al. 2004) for program GS-2008A-Q-205 (PI: Davidge). GMOS is an imaging spectrograph that covers an unvignetted 5.5×5.5 arcmin area on the sky in the 0.36 to $1.1 \mu\text{m}$ wavelength range. The GMOS detector has been updated twice since the instrument was first commissioned roughly two decades ago. At the time these data were recorded the detector was a mosaic of three 2048×4068 EEV CCDs, with a 0.5 mm separation between CCDs. Each pixel subtends 0.073 arcsec on a side. The pixels were binned 2×2 during readout for these observations.

This was a Band 4 program (i.e. a program intended for poor observing conditions) that requested as many observations as possible. By virtue of its Band 4 status it was executed when the image quality was at best fair, and the delivered image quality typically fell between 1.0 and 1.5 arcsec full-width at half maximum (FWHM), with an upper limit of 1.6 arcsec FWHM. The environmental conditions defined for the program specified that observing be limited to no more than light cloud cover, and so there are modest night-to-night variations in transparency. Only one night of observations was deemed unuseable, and this was due to extremely high background light levels. Given that the data were not always recorded during photometric conditions, all images were calibrated to a common photometric reference that was defined by the CFHT MegaCam images discussed by Davidge (2006).

An observing sequence for each night consisted of a series of g' exposures that each had a 300 second integration time. The telescope was offset by a few arcsec between exposures. A log of the observations is provided in Table 1, where the date of observation, the number of exposures recorded per night, and the FWHM category (see below) measured from the point spread function (PSF) in the final processed image for each night are listed. All but one of the images with poorer image quality were recorded during July 2008.

The observations were processed with a standard pipeline for CCD images at visible and blue wavelengths. The required calibrations were recorded throughout the June 2008 to January 2009 time frame. The two primary processing steps were bias subtraction and flat-fielding, with the latter done using observations of twilight sky. The bias-subtracted and flat-fielded exposures recorded on each night were aligned to correct for dither offsets and then averaged together. Any exposures that had obvious departures in image quality and/or

Date (UT)	# of Exposures	FWHM Category (arcsec)
June 28 2008	21	1.0
June 30 2008	16	1.5
July 02 2008	14	1.5
July 07 2008	21	1.0
July 09 2008	11	1.0
July 10 2008	15	1.5
July 11 2008	21	1.5
July 17 2008	6	1.5
July 19 2008	30	1.5
July 25 2008	37	1.5
July 28 2008	9	1.5
Sept 01 2008	11	1.0
Sept 08 2008	11	1.0
Sept 10 2008	22	1.0
Oct 07 2008	3	1.0
Jan 04 2009	24	1.0
Jan 05 2009	6	1.0
Jan 06 2009	18	1.0

Table 1: GMOS Observations

transparency for that night were not included when constructing nightly means.

2.2. Archival Observations

Observations from other facilities are used to expand the time coverage and extract broad-band colors. Extending the time coverage is of particular interest among variable stars with light variations that occur over multi-year time scales and/or in an erratic manner. Colors are also of obvious interest to characterize the variables. Relevant properties of the archival datasets are summarized in Table 2. A brief discussion of each supplemental dataset is provided in the following sub-sections.

Instrument	Filters	Dates (UT)	Program ID
CFHT MegaCam	g', r', i'	12/23/2003	03BC03
	g'	11/20/2003	
CTIO DECam	g^a	11/06/2015	2012B-0001
SPITZER IRAC	[3.6],[4.5]	03/18/2014 10/10/2014	57359

Table 2: Archival Data

^aObservations in other filters were obtained with DECam, but these are not considered in this paper as they were recorded during non-photometric conditions.

2.2.1. *MegaCam*

Images of NGC 247 in g' , r' , and i' were recorded with the CFHT MegaCam (Boulade et al. 2003) on December 23, 2003. These data were discussed previously by Davidge (2006), and were recorded ~ 3 years before the GMOS observations, thereby allowing long term trends in brightness to be examined. These images were also recorded during photometric conditions and have an angular resolution that is comparable to that of the GMOS images. Therefore, they are well-suited for setting the photometric calibration of the GMOS data. The use of a common photometric reference also means that the identification of variables is

done in a pseudo-differential – as opposed to absolute – manner. As the MegaCam images of NGC 247 were all recorded on the same night then they can be used to measure colors at a single epoch that are free of phase-related variations.

MegaCam g' observations of NGC 247 were also recorded on November 20, 2003. These were not considered by Davidge (2006) as they did not pass the seeing requirements specified in the original proposal. Still, these data can be used to obtain photometry of the variables, and further expand the time coverage. Both sets of MegaCam images were processed with the ELIXIR pipeline (Magnier & Cuillandre 2004).

2.2.2. *DECam*

Images of NGC 247 were recorded in g with the CTIO DECam (Flaugh et al. 2015) in 2015 as part of program 2012B-0001 (PI: Frieman). The DECam images were recorded ~ 7 years after the GMOS observations, and so provide important constraints on long-term variability. Processed version of the DECam images were downloaded from the NOIRLab archive.

When compared with the other observations used in this paper, the DECam data have a short exposure time (90 seconds in g). These data were also recorded during non-photometric conditions when the seeing was poor, with FWHM ~ 2 arcsec. The photometric calibration of the DECam g data was set using the same measurements obtained from the CFHT MegaCam observations that were used to calibrate the GMOS observations. Observations of NGC 247 were also recorded with DECam through other filters. However, given the indifferent image quality and the non-photometric conditions, the observations recorded with DECam through those filters were not considered.

2.2.3. *IRAC*

[3.6] and [4.5] images of NGC 247 were obtained with the SPITZER (Werner et al. 2004) IRAC (Fazio et al. 2004) as part of the SPIRITS survey (Kasliwal et al. 2017). Observations at these wavelengths are of interest to characterize the IR SEDs of variables and identify objects that might have warm circumstellar dust shells. The images from the SPIRITS survey sample a number of epochs, and the two datasets recorded in 2014 with astronomical observation request identifiers 50548736 and 50548992 that were discussed by Davidge (2021) were adopted for the present work. The processing of these data was discussed by Davidge (2021).

3. PHOTOMETRIC MEASUREMENTS AND VARIABLE STAR IDENTIFICATION

3.1. Photometry

The distribution of FWHMs among the nightly images is approximately bimodal, with peaks near 1 arcsec and 1.5 arcsec. That the FWHMs typically equal or exceed 1 arcsec is due to the relaxed nature of the requested observing conditions, which are a defining characteristic of Gemini Band 4 programs. Given the bimodal distribution of FWHM values, the images were divided into two groups. One group (images with $\text{FWHM} \sim 1 \text{ arcsec}$) constitute the core dataset for the identification of variable objects based on the dispersion in their magnitude measurements, while the second group (images with $\text{FWHM} \sim 1.5 \text{ arcsec}$) provide supplementary photometric measurements of variable stars that were identified in the first group. The FWHM classification of the images recorded on each night is listed in Table 1. All of the images in the 1.5 arcsec FWHM group were recorded in July 2008.

A median image of all frames in the 1 arcsec FWHM group was constructed after adjusting for frame-to-frame differences in sky transparency, and the result served as a reference for photometric measurements and the assessment of variability. As it is constructed from ten frames, the statistical noise throughout much of the median image is lower than in individual frames. However, source confusion is by far the dominant obstacle for detecting stars in dense parts of the NGC 247 disk.

Stellar brightnesses were measured with the PSF fitting program ALLSTAR (Stetson 1994). Tasks in DAOPHOT (Stetson 1987) were used to identify stars, estimate preliminary magnitudes, and construct the PSF from a sample of bright, isolated stars. The photometric calibration is based on the brightnesses of isolated stars with magnitudes measured from the CFHT MegaCam g' image.

Unresolved stars in NGC 247 form a complex background that complicates stellar photometry, and light from this background was removed using an iterative process. First, an initial set of photometric measurements was obtained with the background light in place. The photometered stars were subtracted from the initial image, and the result was smoothed with a median filter to suppress artifacts of the subtraction process. The resulting smoothed image tracks the light from unresolved stars, and was subtracted from the initial image to produce an image in which unresolved light has been removed. Final photometric measurements were then made from the background-subtracted image.

The source catalogue obtained from the median image was adopted for photometry on each of the nightly images. A potential shortcoming of the use of such a master source

catalogue is that eruptive variables such as novae and background supernovae that fall above the detection limit on only some nights will likely be missed. However, a benefit is that all of the variables found should be recoverable in images recorded at other epochs, and this is borne out in the high recovery rate of variables in the MegaCam and DECam images (see below) that were recorded years before/after the GMOS observations.

The brightnesses of sources in the MegaCam and DECam images were also measured with ALLSTAR. As the depths and angular resolutions of the MegaCam and DECam images differ from those in the GMOS observations, separate source catalogues were generated for each of these datasets. The brightnesses of variables that were identified from the GMOS observations were then extracted from the MegaCam and DECam photometric catalogues.

3.2. Variable Star Identification Using Dispersion in Photometric Measurements

The dispersion in magnitudes measured over a range of epochs is an obvious criterion for identifying variable stars. In the current study, sources that had a dispersion in night-to-night measurements that departed from the magnitude measured in the 1 arcsec FWHM median image at the 5σ or higher significance level were tagged as candidate variables. The threshold dispersion was set by calculating the night-to-night scatter in the brightnesses of stars having similar magnitudes, but with σ -clipping applied to reject variable stars. There are numerous other criteria for selecting variables, and in Section 6 the sample of variable stars is expanded further by applying slightly relaxed detection criteria in a region of the CMD associated with LBVs.

While dispersion in the photometry is the primary criterion for identification as a variable star in this section, other constraints were also imposed. Candidate variables had to be detected in all ten of the 1 arcsec FWHM images. In addition, the images were inspected to identify objects where the photometry might be skewed by diffraction spikes from very bright stars, as well as transient events such as cosmic rays or trails from minor planets and artificial satellites. Finally, objects that were located in or close to the gaps between CCDs or were close to the detector edges were removed from the sample.

While a 5σ criterion that also requires detection in all ten 1 arcsec FWHM images sets a high threshold for selection, it ensures (1) that the light variations in the final sample are not the result of statistical fluctuations in the photometric measurements, and (2) that a light curve could be constructed with at least ten points. The strict identification criteria also facilitate the detection of variables in the archival datasets, and all of the variables

discovered in this study were recovered in at least one of the two MegaCam g images. Two of the brightest variables were saturated in the December 2003 g image, and so were not recovered with those data. All but one of the faintest variables was recovered from the DECam g observations.

The photometry of the variables that were identified from the 1 arcsec images was supplemented with photometric measurements made from the 1.5 arcsec FWHM images. The faint limits of the 1.5 arcsec FWHM images tend to be a few tenths of a magnitude brighter than that of the 1 arcsec FWHM images, and sources that are close to the faint limit of the 1 arcsec images when they are near the low point of their light variations were not recovered in some of the 1.5 arcsec FWHM images. Still, the majority of variables found here are bright enough that measurements made from the 1.5 arcsec images tend not to contribute additional scatter to the light curves.

The co-ordinates and photometric properties of the variables identified using the procedures described above are listed in Table 3. The co-ordinates were obtained from the world co-ordinate system information in the GMOS image headers. The co-ordinates measured from bright stars in the GMOS image are consistent with those in the 2MASS Large Galaxy Atlas (Jarrett et al. 2003) image of NGC 247 to within 1 – 2 arcsec, suggesting that the co-ordinates in Table 3 are reliable to ± 2 arcsec. The magnitudes listed in Table 3 are from the 1 arcsec FWHM median image, and so are ‘typical’ brightnesses during the second half of 2008. The periods and light curve types listed in Table 3 are discussed in the next section. Finding charts that show the 15×15 arcsec area centered on each variable are shown in Figure 1.

The area observed with GMOS contains a modest number of previously identified variable stars. Two Cepheids (cep011 and cep022) discovered by Garcia-Varela et al. (2008) were recovered using the procedure described above. There is an offset with respect to the Garcia-Varela et al. (2008) co-ordinates of 2 arcsec in declination, and 1 sec (~ 14 arcsec) in right ascension.

Garcia-Varela et al. (2008) found four other Cepheids in the area imaged with GMOS, and these were not recovered independently with the GMOS observations. One of these (cep013) was missed because of its proximity to the edge of the GMOS science field. An examination of the GMOS photometry of this object reveals variations in its brightness that exceed the 5σ detection criterion as well as a light curve that is consistent with Cepheid variability. Thus, it would have been detected if it were further from the edge of the GMOS science field. Lacking finder charts, we have not been able to identify unambiguously the other three previously-detected variables (cep008, cep016, and cep018) in the median g' image, and so the brightness variations in the GMOS data can not be examined to assess

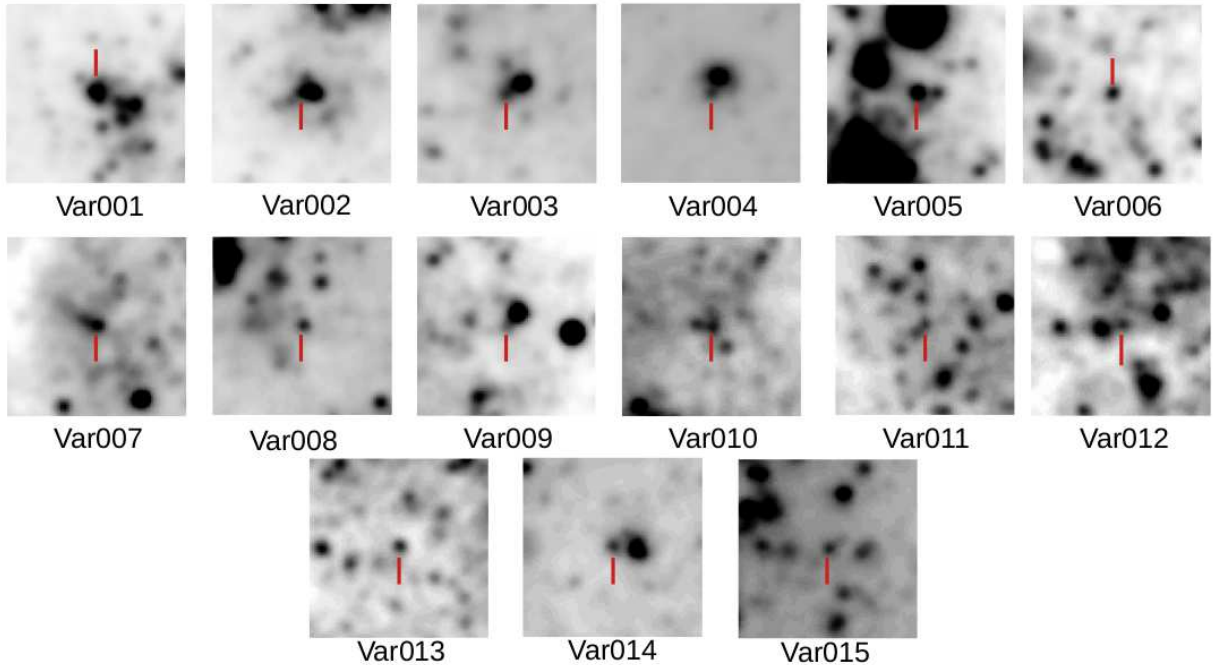


Fig. 1.— Finding charts for the variables listed in Table 3, which were identified using the 5σ dispersion criterion discussed in Section 3. Each image is 15×15 arcsec on a side, with North at the top and East to the right. The variable stars are centered in each frame, and are at the end of the red line. These images were extracted from the median g' 1 arcsec FWHM image.

ID	RA (2000)	Dec (2000)	g' ^a	Period (days)	Type ^b	Other Names
Var001	00:47:15.4	−20:47:35	20.2		cLBV	
Var002	00:47:00.7	−20:46:39	21.5		SRb	
Var003	00:47:05.8	−20:48:05	21.5		cLBV	
Var004	00:47:08.8	−20:50:56	21.1		BV	
Var005	00:47:10.5	−20:48:50	21.6	13.0?	cLBV	
Var006	00:47:12.7	−20:50:00	21.7	33.3?	CBS?	
Var007	00:47:08.7	−20:47:16	21.8		SRb	
Var008	00:47:10.3	−20:51:14	22.0	73.3	Cep	cep022
Var009	00:47:11.3	−20:49:01	22.5		cLBV	
Var010	00:47:11.5	−20:48:47	22.7	33.2	Cep	cep011
Var011	00:47:04.8	−20:49:45	23.6		SRb	
Var012	00:47:09.0	−20:48:24	23.2		SRd	
Var013	00:47:10.5	−20:50:20	22.9	22.9	Cep	
Var014	00:47:16.3	−20:50:26	22.7	22.5	Cep	
Var015	00:47:17.7	−20:47:48	23.1	20.3	Cep	

Table 3: Variables Detected Using the Dispersion in the Photometric Measurements

^aMagnitude measured from the median 1 arcsec FWHM g' GMOS image.

^bcLBV = candidate luminous blue variable; SR = semi-regular variable; Cep = Cepheid; CBS = close binary system.

why these stars evaded detection. We suspect that the failure to independently recover these variables is due to the shorter time coverage of the GMOS data (7 months for GMOS versus up to 2.3 years for the data used by Garcia-Varela et al. 2008), coupled with stochastic effects when sampling their light curves.

Four of the stars in Table 3 are classified as candidate LBVs (cLBVs), and this classification should be regarded only as a place-holder. *Bona fide* LBVs form a diverse group of objects (reviews by Humphreys & Davidson 1994 and Smith 2014), and are just one type of intrinsically bright blue variable star. Humphreys & Davidson (1994) review the photometric properties of LBVs, and identify four distinct time scales for variations, with the largest amplitude variations occurring over time scales of decades or centuries. Barring a fluke detection of such a multi-magnitude eruption from an LBV, the observations discussed here will more likely detect the variations on the order of a few tenths of a magnitude that are seen over timescales of a few months to years in the light curves of some LBVs. Martin

& Humphreys (2017) examine the photometric properties of LBVs and candidate LBVs in M33 over a five year baseline and find 0.1 - 0.8 magnitude spreads in V . Other types of intrinsically bright blue variables show a similar range in V magnitudes.

Solovyeva et al. (2020) examined spectra and photometry of two luminous early-type stars, and both are in the area of NGC 247 that was observed with GMOS. One of these (J004703.27-204708.4) was not detected as a variable in the present study using the 5σ criterion described in this section, although evidence is presented for moderate variability in the light curve of this star in Section 6. The other star fell in the gap between CCDs in the GMOS detector, and so has uncertain photometry.

4. LIGHT CURVES, PERIODS, AND PHASING

The nightly GMOS magnitude measurements of the sources listed in Table 3 are shown in Figure 2. The random uncertainties in the individual measurements are typically a few hundredths of a magnitude, and it should be recalled (Section 3.2) that a criterion for selecting objects as variables was that the dispersion in the various measurements exceed this at the 5σ level. The dispersion in the measurements that allowed these objects to be flagged as variables is thus clearly evident. These light curves were used to sort the sample into two groups: (1) obvious periodic variables, and (2) objects that are either non-periodic or that have a period that can not be determined from the existing data. The objects in each group are discussed in the following sub-sections.

4.1. Periodic and Possibly Periodic Variables

The periods of some stars can be determined directly from the measurements in Figure 2. The phased light curves of these stars, constructed with the periods listed in Table 3, are shown in Figure 3. As these are a disparate group of objects then zero phase coincides with the first date that images were recorded with GMOS (June 28, 2008).

The phased light curves of five of the stars (Var008, Var010, Var013, Var014, Var015) coupled with their broad-band colors (Section 5) suggest that they are classical Cepheids. The two brightest Cepheids identified from the GMOS images were also identified by Garcia-Varela et al. (2008), and these are stars cep011 and cep022 in their Table 5. The three faintest Cepheids in our sample were not detected by Garcia-Valera et al. (2008). These likely evaded detection in that study because they are faint and in moderately crowded environments. Cepheids with similar periods were discovered by Garcia-Valera et al. (2008),

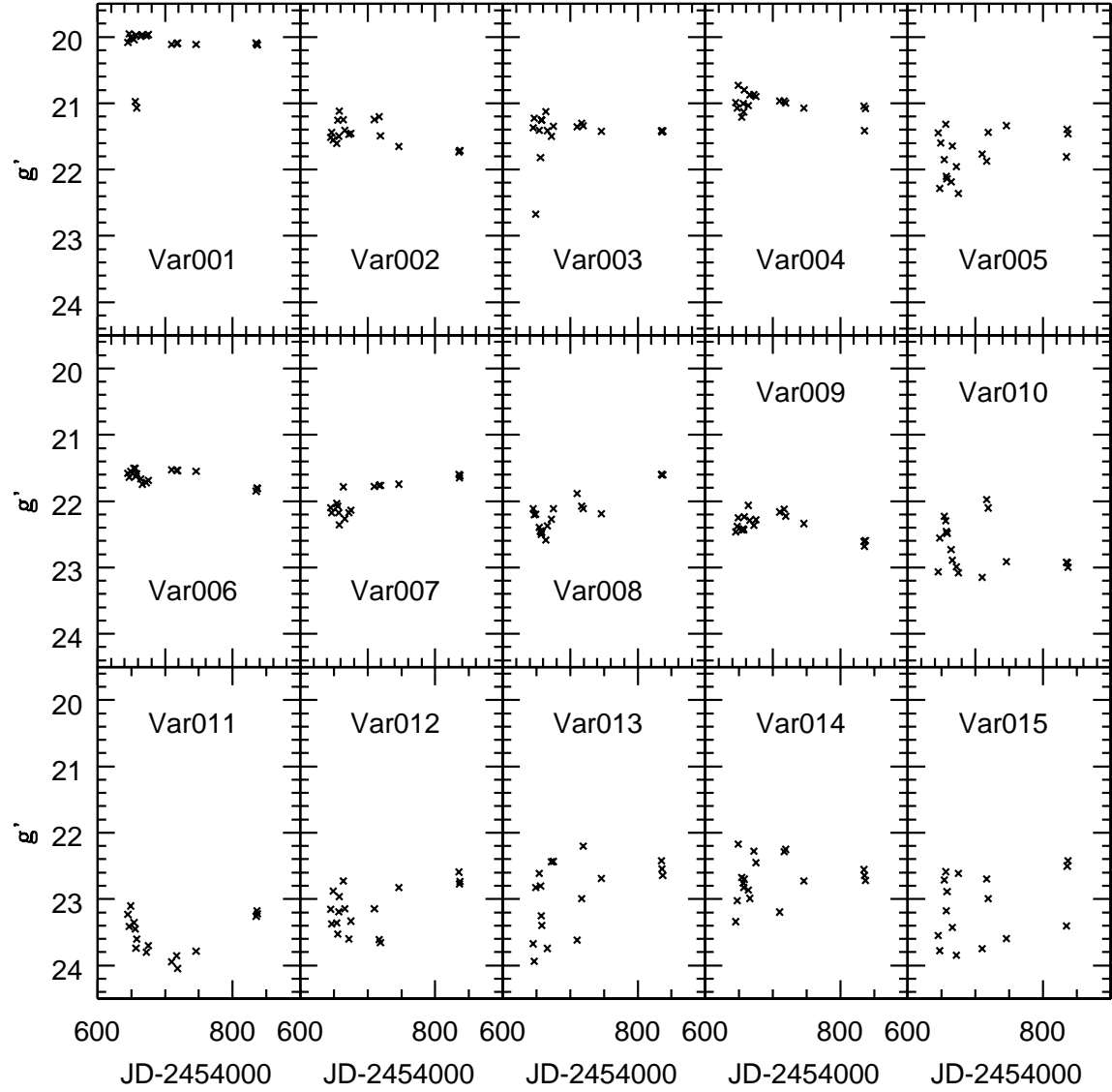


Fig. 2.— Unphased light curves of the variable sources that were identified using the dispersion criterion in Section 3. Only measurements made from the GMOS images are shown to highlight the variations in brightness that served as the basis for their identification as *bona fide* variables. The random uncertainties in individual measurements is typically a few hundredths of a magnitude, and so is – by definition (Section 3.2) – much smaller than the amplitude of the light variations. Some of the light curves show signs of periodic behaviour, while others show no evidence of periodicity in the time interval sampled with GMOS.

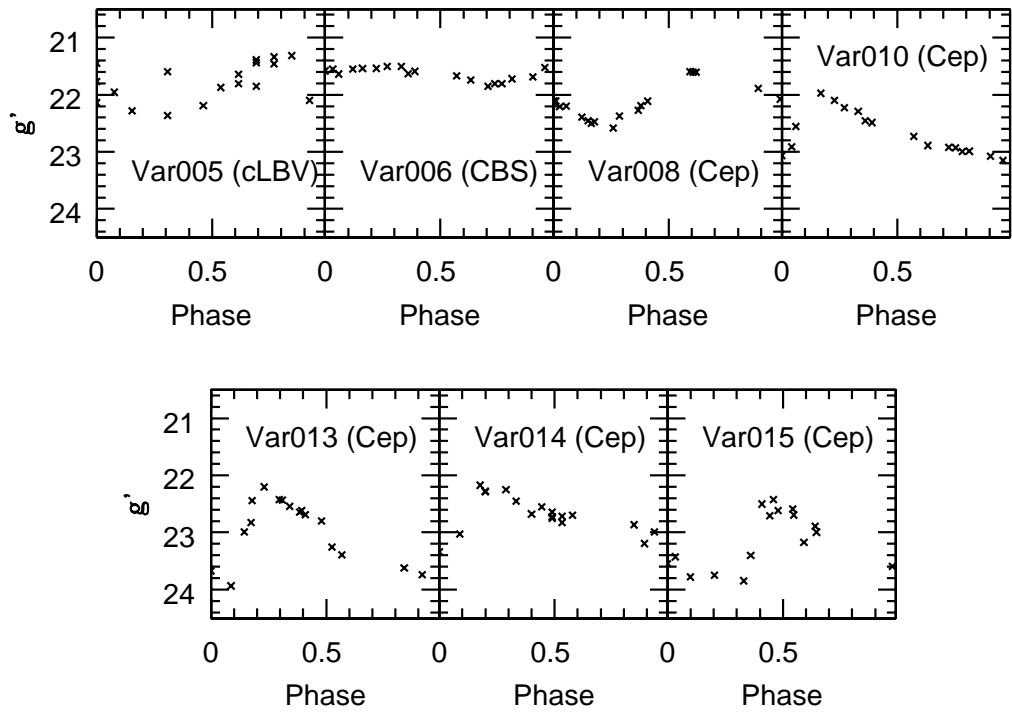


Fig. 3.— Phased light curves. Given the disparate nature of the variables, phase zero coincides with June 28, 2008 (i.e. the first date of observation with GMOS). The light curves of Var008, Var014, Var013, Var010, and Var015 are indicative of classical Cepheids. Based in large part on its location in the CMD we suggest that Var006 is a CBS. Var005 is included in this figure given the periodic nature of its light variations in Figure 2. However, the scatter in the light curve indicates that the period estimated for Var005 is highly uncertain, and this star is classified as a candidate LBV.

but in the northern parts of NGC 247, where the stellar density tends to be lower than in the south.

The light curve of Var006 in Figure 2 shows periodic low amplitude variations. While the phased light curve of Var006 is reminiscent of that of a Cepheid with a broadened maximum, it is likely not a Cepheid. It is near the bright end of stars in our sample, and the 33.3 day period is shorter than might be expected for an intrinsically bright Cepheid, although the difference in magnitude between Var006 and Var008 is within the ± 0.5 mag scatter (Storm et al. 2011) in the period-luminosity relation. The light curve of this star also has a modest amplitude when compared with that of other Cepheids. Most importantly, in Section 5 it is shown that its location in the CMD places it well blueward of the Cepheid instability strip, making it an object with an early spectral type.

While not shown in Figure 2, the MegaCam and DECam observations indicate magnitudes that are consistent with those made with GMOS, and so there is no evidence for large amplitude variations over timescales of many years. This leads us to conclude that while Var006 is a bright early-type variable, it is likely not a LBV as it is also well below the S Dor instability strip (Section 5). Given the low amplitude, periodic nature of the light variations, we suggest that Var006 is a close binary system (CBS), with the light variations due to temperature variations on one star in a contact or near-contact binary system. The inclination of the system is such that eclipses do not occur. A massive CBS interpretation is consistent with a system of two stars with $M_V \sim -5.5$, and a spectroscopic search for signatures of two stars would confirm or negate this possibility. If it is a massive system undergoing mass transfer then spectra might also reveal signatures of system-wide mass loss due to mass flow through the L_2 Lagrangian point (e.g. Webbink 1976).

Despite showing hints of periodic variations in Figure 2, the phased light curve of Var005 in Figure 3 suggests that these may only be short-lived quasi-periodic variations. There is considerable scatter in the phased light curve of this star, indicating that the 13 day period estimate is uncertain, even though it appears to be moderately well constrained by the July 2008 observations. Var005 is one of the brightest variables identified here, and has colors that are indicative of an early-type star. The location of Var005 on the CMD constructed from the MegaCam observations is ~ 1 magnitude below the S Dor instability strip (Section 5). However, it is ~ 1.5 magnitudes brighter in the GMOS observations, placing it in the region occupied by LBVs. Hence, we suggest that it is a candidate LBV that had quasi-periodic variations in June and July 2008.

4.2. Semi-regular and Non-periodic Variables

Light curves of the sources that do not show evidence of clear periodicity in the GMOS observations are shown in Figure 4. DECam and MegaCam measurements are also shown so that trends over decadal timescales can be examined. Based on these light curves, combined with locations in the CMD (Section 5), these are identified as probable semi-regular red and yellow supergiant variables, while others are potential LBVs.

There are episodic variations in the GMOS light curve of Var002 in Figure 2, with considerable night-to-night scatter. The amplitude of the light variation increases with the inclusion of photometry from the MegaCam and DECam images, and there is a clear long-term trend in brightness in Figure 4. Var002 has one of the reddest $g' - i'$ colors (next section). The photometric characteristics are consistent with light variations from supergiants that show semi-regular light variations. We thus classify Var002 SRb.

The light curve of Var011 is unique among the variables found in this paper. There is a 0.8 magnitude decline in light level over a time span of tens of days in the GMOS observations, although at the end of the ~ 200 day GMOS observation sequence the light level had recovered to its initial value. The MegaCam and DECam brightnesses of this star in Figure 4 indicate that the initial and final light levels in the GMOS data are ‘typical’ brightnesses for this star.

Light variations of this nature and duration are reminiscent of those in R CrB stars. The dominant features in the light curves of classic R CrB variables are multi-magnitude dips in light levels over long time spans. These are accompanied by frequent dips in brightness that amount to a few tenths of a magnitude. The large scale variations in light levels are thought to be due to extinction by dust, while the more modest variations may be due to pulsations (e.g. Clayton 1996). R CrB stars are H-deficient supergiants with a typical intrinsic magnitude $M_V \sim -5.5$, and so such a star in NGC 247 should have $g \sim 22.5$, which is consistent with the measured brightness of Var011 outside of the light dip seen here. A potential problem with the R CrB interpretation for Var011 is that these stars have excess IR emission from circumstellar dust (e.g. Lambert et al. 2001). The [3.6]–[4.5] color of Var011 does not show signs of an IR excess (Section 5), suggesting that if hot dust is present then it does not dominate the signal at these wavelengths. The nature of the variability observed in Var011 is thus not clear. Spectra would reveal if this star is deficient in Hydrogen.

The light variations of Var012 in Figure 3 are suggestive of periodic activity, although a period could not be found with these data. If the observations are restricted to those recorded in June – July 2008 then a Cepheid-like light curve with a 14 – 17 day period is found, with preference for longer periods. However, when the entirety of the 7 month GMOS

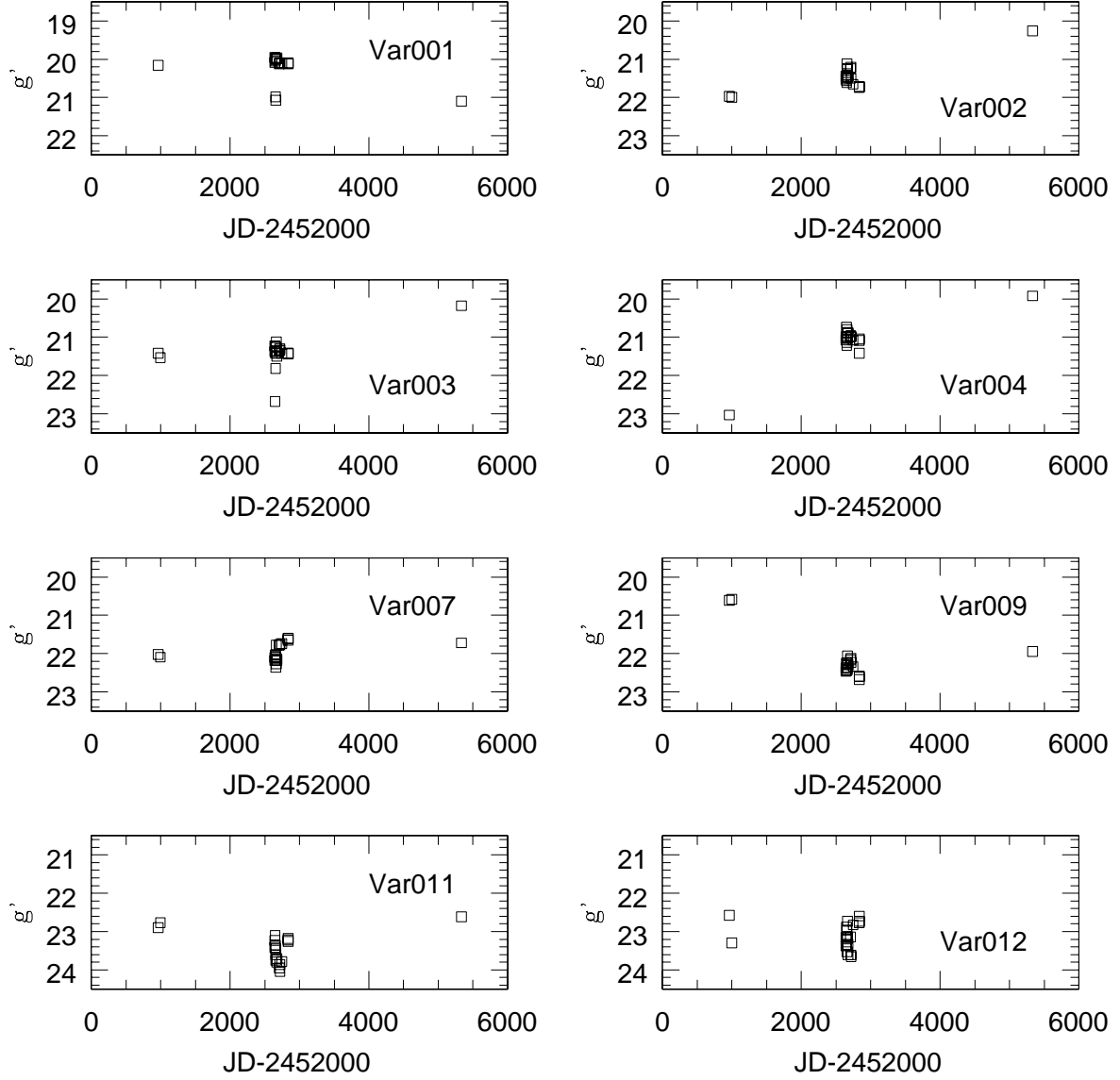


Fig. 4.— Unphased light curves of variables without periods. Photometry from the 2003 MegaCam observations and the 2015 DECam observations are also shown. The scatter in the GMOS measurements that served as the basis for the identification of these objects as variables is clearly evident. The inclusion of the MegaCam and DECam photometry reveals trends in visible light that extend over decade-long timescales in the light curves of Var002, Var003, Var004, and Var009.

dataset is considered the construction of a well-defined phased light curve is elusive. There is a ~ 0.6 magnitude difference in the November and December 2003 MegaCam observations in Figure 4, and this is comparable to the dispersion in the GMOS observations, hinting that the amplitude seen in the GMOS observations is at least stable, if not periodic. Based on these light variations we suggest that Var012 is a semi-regular variable. The location on the CMD places it near the blue edge of the Cepheid instability strip (Section 5), leading to a proposed classification of SRd.

Multi-year trends in brightness are seen in the light curves of Var001, Var003, Var004, and Var009 in Figure 4. All have blue $g' - i'$ colors, and are intrinsically bright sources at visible/red wavelengths. The light curves of Var001 and Var003 show ~ 1 magnitude drops at two different epochs in the GMOS data, while Var009 shows a slower paced drop in its light level in Figure 2. Var004 shows a steady increase in brightness throughout the 12 year time span bracketed by the MegaCam and DECam images.

The blue variables tend to be in complex environments with bright nearby neighbors, and so their photometry is prone to night-to-night seeing variations. However, the dips in the light levels in Var003 and Var001 occur on two different nights that had different image qualities. This suggests that these dips are not related to seeing variations, which could affect photometry in crowded areas. The blue variables have mean intrinsic brightnesses $M_V \sim -9$ (Var001), -8 (Var003), -7 (Var004), and -5.5 (Var009) if they are at the distance of NGC 247, and this is consistent with them being massive evolved stars. Based on the location of these objects in the CMD, we classify Var001 and Var003 as *potential* LBVs in Table 3. Var004 and Var009 are classified as blue variables - these objects are likely evolved massive stars that are not LBVs.

5. PHOTOMETRIC PROPERTIES: LOCATIONS IN CMDS AND ON THE SKY

The archival observations described in Section 2 span a broad range of wavelengths, and can be used to place the variable stars on a CMD, albeit with photometry that samples only one epoch. Not only do photometric measurements that span a range of wavelengths provide clues into the nature of the variables, but they can also be used to examine their immediate environment; for example, the detection of IR excess radiation could be suggestive of mass deposition into a circumstellar envelope. Further insights into the nature of the variables, including their evolutionary state and physical characteristics, can be gleaned by examining their locations in NGC 247, such as proximity to star-forming regions.

Photometric measurements of the variables taken from the MegaCam and IRAC images are compiled in Table 4. The majority of measurements at visible/red wavelengths are from the December 2003 MegaCam images and give colors only at that epoch. The SEDs of variables will likely change with phase, and the MegaCam and IRAC images do not sample the same phase. The 1σ random uncertainties as estimated by ALLSTAR are shown in brackets beneath the measurements. Uncertainties in the absolute photometric calibration of the MegaCam measurements are on the order of a few hundredths of a magnitude. The intrinsic angular resolution of the SPITZER images is poorer than that of the MegaCam observations. The potential for blending, especially in compact star forming regions that contain the candidate LBVs, thus should not be discounted. Five variables were not recovered in the SPITZER images.

5.1. CMDs and IR Colors

The locations of the variables on the $(i', g' - i')$ CMD are indicated in Figure 5, where magnitudes and colors from the December 2003 MegaCam observations are shown. Areas of the CMD that are expected to contain Cepheids and LBVs are also marked. The Cepheid instability strip in Figure 5 is that specified by Di Criscienzo et al. (2013), and the variables identified here as Cepheids fall within its boundaries. The blue and red boundaries of the region that contains LBVs shown in Figure 1 of Smith et al. (2004) are also indicated in Figure 5. The area of the CMD that contains LBVs appears to extend to fainter magnitudes than the classical S Dor strip (Smith et al. 2019). The blue S Dor sequence coincides with a discontinuity in the NGC 247 CMD. The two most luminous LBV candidates found from the GMOS observations using the dispersion in the magnitude measurements have intrinsic colors and magnitudes that place them on the S Dor instability strip, although spectra will be required to assign these secure LBV designations.

The expected brightness of the S Dor strip in Figure 5 is consistent with the brightnesses of LBVs in other galaxies that have similar M_K as NGC 247, and hence likely have similar metallicities. M33 is of particular interest as it has a well-populated intrinsically bright blue plume in its CMD, and a number of LBVs and candidate LBVs have been identified (e.g. Massey et al. 2007; Humphreys et al. 2017 and references therein). These have V between 16 and 18 (Martin & Humphreys 2017), which corresponds to $V \sim 19.5 - 21.5$ at the distance of NGC 247. Given that the g' and V magnitudes of blue stars differ by only a few tenths of a magnitude (Fukugita et al. 1996) then the LBV population of M33 thus overlaps with the area in Figure 5 that is expected to contain LBVs after accounting for the difference in distance.

ID	g^a	$g^a - r^a$	$r^a - i^a$	$[3.6] - [4.5]^b$	$g' - [3.6]$
Var001	20.192 (± 0.02)	-0.064 (± 0.03)	0.075 (± 0.03)	-0.02 (± 0.07)	4.04 (± 0.07)
Var002	21.968 (± 0.03)	0.849 (± 0.03)	0.934 (± 0.03)	-0.07 (± 0.10)	5.52 (± 0.10)
Var003	21.510 (± 0.03)	0.166 (± 0.05)	-0.543 (± 0.04)	0.38 (± 0.08)	5.31 (± 0.08)
Var004	23.052 (± 0.12)	-0.305 (± 0.12)	-0.758 (± 0.19)	–	–
Var005	21.344 (± 0.01)	-0.302 (± 0.01)	-0.222 (± 0.03)	–	–
Var006	21.767 (± 0.01)	-0.145 (± 0.02)	-0.017 (± 0.02)	–	–
Var007	22.053 (± 0.04)	1.264 (± 0.03)	0.800 (± 0.03)	0.31 (± 0.13)	5.23 (± 0.13)
Var008	21.634 (± 0.01)	0.523 (± 0.02)	0.094 (± 0.02)	–	–
Var009	20.566 (± 0.01)	-0.237 (± 0.01)	-0.151 (± 0.01)	0.13 (± 0.08)	4.27 (± 0.08)
Var010	22.466 (± 0.02)	0.566 (± 0.02)	0.264 (± 0.02)	-0.29 (± 0.15)	5.52 (± 0.15)
Var011	22.760 (± 0.03)	1.283 (± 0.03)	0.702 (± 0.03)	0.09 (± 0.25)	4.68 (± 0.25)
Var012	23.240 (± 0.05)	0.230 (± 0.06)	0.279 (± 0.06)	0.38 (± 0.20)	5.82 (± 0.20)
Var013	22.973 (± 0.02)	0.588 (± 0.03)	0.545 (± 0.03)	–	–
Var014	23.240 (~ 0.03)	0.590 (± 0.03)	0.345 (± 0.04)	-0.15 (± 0.25)	5.15 (± 0.25)
Var015	23.799 (± 0.05)	0.776 (± 0.05)	0.272 (± 0.05)	-0.04 (± 0.18)	6.41 (± 0.18)

Table 4: Multi-wavelength Measurements

^aMeasured from December 23, 2003 MegaCam images.

^bMeasured from mean of IRAC images recorded on March 18, 2014 and October 10, 2014.

NGC 2403 is a late-type spiral galaxy in the M81 group with a distance modulus similar to that of NGC 247, and the LBVs V37 and V38 in that galaxy have $V = 20.6$ and 19.4, respectively (Humphreys et al. 2019). As with the LBVs in M33, the brightnesses of these objects overlap with the area marked in Figure 5 that is expected to contain LBVs. We emphasize that the region of the CMD that contains LBVs also contains other types of intrinsically bright blue variables (e.g. Martin & Humphreys 2017), so a location on the CMD that is close to the S Dor instability strip is not an ironclad indicator of a classification as an LBV.

Because they encompass a diverse group of objects, semi-regular variables are found over a range of locations in the CMD. Var012 falls near the blue edge of the Cepheid instability strip. As discussed previously, a secure period could not be identified for this star, leading us to assign it class SRd. As for the other semi-regular variables, these fall at or near the bright end of the red plume in the CMD, as expected if they are heavily evolved supergiants. The absence of periodicity suggests a classification of type SRb for these stars. At least some of these stars have well known analogs in the Galaxy. The classical semi-regular variable star Betelgeuse (α Ori) has $M_{i'} \sim -8$, which would correspond to $i' \sim 20$ in NGC 247. This is comparable to the brightest semi-regular red variables detected here.

Davidge (2021) discussed the $([3.6], [3.6]-[4.5])$ CMD of NGC 247. The peak of the stellar sequence in NGC 247 was found to occur near $[3.6] = 17$ based on a comparison of number counts in NGC 247 with those in a control field that is offset from the galaxy. Intrinsically rare sources in NGC 247 might then be brighter than $[3.6] = 17$, given that they may not occur in numbers that would elevate them in a statistically significant manner above those of foreground and background objects. In fact, the entries in Table 4 indicate that all three of the candidate LBVs that are detected by SPITZER are brighter than $[3.6] = 17$, reflecting the highly evolved nature and intrinsic luminosity of these stars. In contrast, all of the Cepheids detected in the SPITZER observations have $[3.6]$ magnitudes that are comparable to or below the brightness limit estimated by Davidge (2021) – the brightest of the Cepheids detected by SPITZER is Var010, for which $[3.6] = 16.95$.

$[3.6]-[4.5]$ and $g'-[3.6]$ colors are listed in the last two columns of Table 4. $[3.6]-[4.5]$ colors that exceed those produced by stellar photospheres are a signature of hot dust emission, and none of the variables have $[3.6]-[4.5]$ colors that depart significantly from the scatter envelope of the NGC 247 stellar sequence in Figure 6 of Davidge (2021). With the caveat that the SPITZER and MegaCam observations were not recorded at the same epoch, it is also apparent that the $g' - [3.6]$ colors of the candidate LBVs are not markedly redder than those of the other stars in the sample. Additional evidence for the pedestrian infrared photometric properties of the candidate LBVs in NGC 247 comes in the form of the

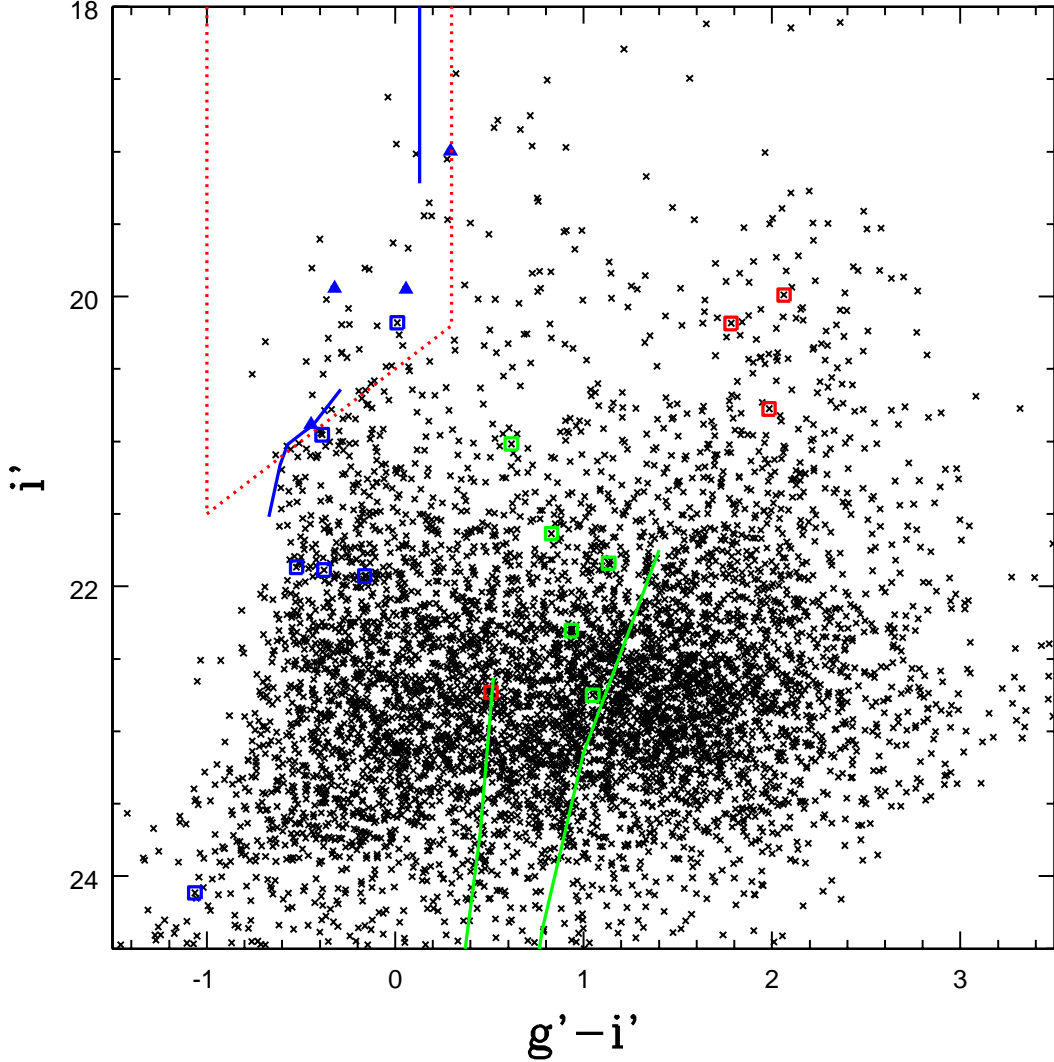


Fig. 5.— $(i', g' - i')$ CMD of stars in the southern half of NGC 247 constructed from the December 2003 MegaCam observations. The locations of all variables found in this paper are marked. Early-type variables (blue squares), Cepheids (green squares), and semi-regular variables (red squares) identified using the procedure described in Section 3 are indicated with open symbols. The four early-type variables identified using location in the CMD in Section 6 are shown as solid blue triangles. The green lines mark the boundaries of the full Cepheid instability strip from Di Criscienzo et al. (2013). The blue lines mark the region occupied by LBVs in Figure 1 of Smith et al. (2004). The LBV boundaries were translated onto the observational plane using relations from de Jager & Nieuwenhuijzen (1987), Fukugita et al. (1996), and Allen (2000). The red dashed lines indicate the region of the CMD used in Section 6 to isolate possible LBVs. The placement of the fiducial sequences assume a distance modulus of 27.64 and $E(B-V) = 0.18$ (Gieren et al. 2009).

mixed success of detection with SPITZER: three of the candidate LBVs were not detected in the SPITZER images. The photospheric-like IR colors of these stars does not mean that hot dust is absent. Rather, if hot dust is present then the emission is smaller than that produced by the stellar photospheres at these wavelengths. While there is no evidence for an IR excess in the candidate semi-regular variables and LBVs in the SPITZER IRAC observations, the possibility of a cool dust shell around these objects can not be discounted without observations at longer wavelengths.

5.2. Location in NGC 247

The locations of the variables discovered in this paper are shown in Figure 6. The background is the median 1 arcsec FWHM GMOS image that served as the reference for the photometric measurements. The locations of Cepheids are shown in the right hand panel, while those of all other variables are indicated in the left hand panel.

Cepheids and non-Cepheids tend to be located in different parts of NGC 247. The majority of blue and semi-regular variables tend to be in or near collections of stars that are likely star-forming complexes and/or associations. This is consistent with these objects being young massive stars. In fact, Rodriguez et al. (2019) found that many of the most luminous blue stars in this part of NGC 247 fall along a serpentine structure that is associated with the edges of large-scale bubbles (Davidge 2021). The majority of the non-Cepheid variables fall along or are close to this serpentine structure.

The Cepheids tend to be found away from star-forming knots and associations. This is consistent with these objects having ages in excess of tens of Myr, thereby giving them time to diffuse away from their places of birth, and/or for their birth places to have dissolved. There is a selection effect when identifying Cepheids, as shorter period Cepheids as well as those with smaller amplitudes will be more susceptible to blending in dense stellar regions. This being said, shorter period Cepheids have older ages than their brighter, longer period cousins. Therefore, they will have had more time to dissociate from their natal environment and migrate to comparatively low density regions.

6. LIGHT CURVES OF PHOTOMETRICALLY SELECTED LUMINOUS BLUE STARS

The 5σ dispersion criterion for selecting variables that was discussed in Section 3 relies on brightness measurements made from the ten images that have ~ 1 arcsec FWHM angular

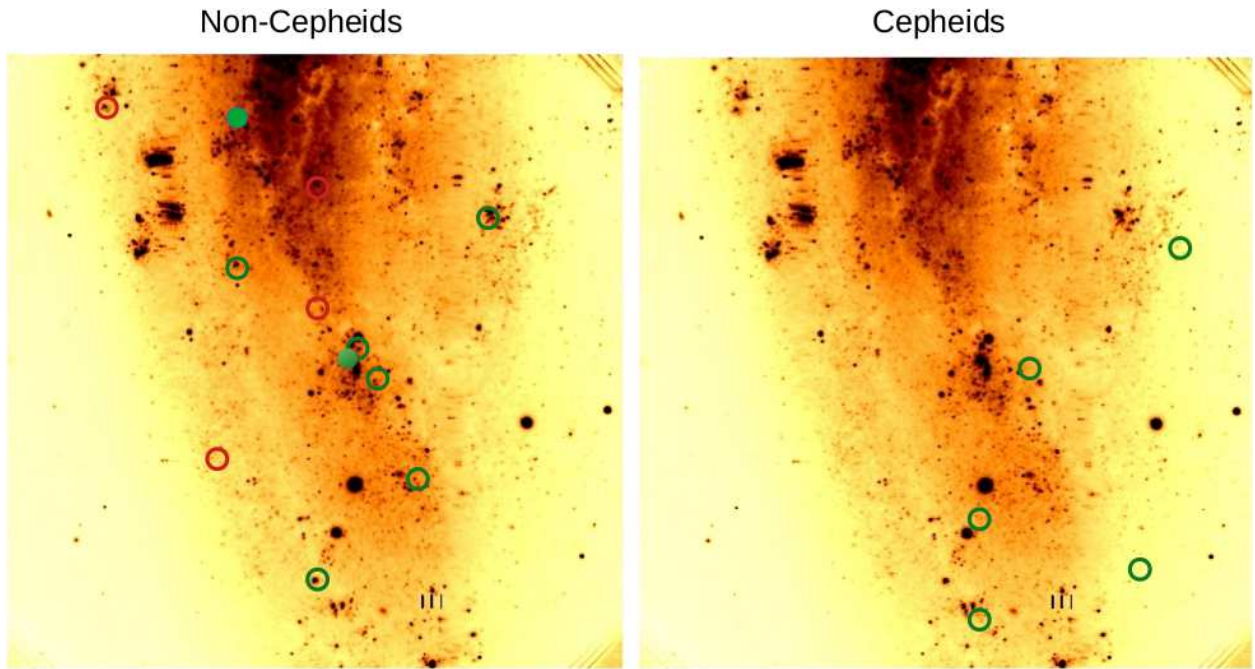


Fig. 6.— Locations of Cepheids (right hand panel) and other variables (left hand panel) in the median 1 arcsec FWHM g' image. Semi-regular variables and candidate LBVs identified using the procedures described in Section 3 are indicated with red and green circles. The locations of the two cLBVs identified using the procedure described in Section 6 are indicated with filled green circles. The Cepheids and non-Cepheids have different locations in the sense that Cepheids tend to avoid star-forming knots, and this is consistent with ages of at least a few tens of Myr. In contrast, many of the semi-regular variables and cLBVs are in star-forming complexes, as might be expected if they are young massive evolved stars.

resolution. While this is a robust means of detecting objects with large amplitude light variations during the course of the observing campaign, it sets a high standard for selecting variables. However, a high standard is necessary to suppress specious detections when large samples of stars are examined.

Another approach is to target sparsely populated locations in the CMD where a high frequency of variables might be expected, as a relaxed criterion for variability can then be applied. Such a procedure might also facilitate the identification of non-periodic and low amplitude eruptive variables – if large scale variability events did not occur when the images with the best image quality were recorded, then these stars may avoid detection when applying the 5σ dispersion threshold discussed in Section 3. It might also be possible to identify subtle long term trends and low amplitude systematic trends in light curves that could evade detection in the dispersion measurements.

The brightest blue stars are obvious targets for pre-selection based on location in the CMD. Many highly evolved massive stars are variable. In addition, the expected contamination from foreground objects will also be modest if one focuses on blue colors. Proximity to the location of star-forming regions provides an additional means of restricting contamination from sources not associated with the target galaxy, while obvious background galaxies with blue colors can also be identified based on their appearance. Finally, because they are among the brightest objects in a galaxy, luminous blue stars also have photometric measurements with comparatively high S/N ratios – low amplitude variations in light might be found that would go undetected in other, fainter stars in the same galaxy.

6.1. Photometry of a Known Bright Blue Variable in NGC 247

Before applying this approach to search for variability in the brightest blue stars, we first examine the photometric properties of a previously studied luminous star in NGC 247. Solovyeva et al. (2020) used spectra and photometry to identify a candidate LBV in NGC 247 (J004702.18–204739.9), as well as a B[e] supergiant (J004703.27–204708.4). The light curve of the former shows evidence of episodic variations with a ~ 1 magnitude amplitude in Figure 4 of Solovyeva et al. (2020), whereas that of the latter varies by $\sim 0.2 – 0.3$ mag in V . Unfortunately, J004702.18–204739.9 falls in one of the gaps between the GMOS CCDs and so reliable photometry of that star can not be extracted from the GMOS images. However, reliable photometry can be obtained for J004703.27–204708.4. The GMOS photometry is of interest for that star as it samples a portion of the light curve not covered previously. Perhaps of greater relevance for the present study is that the sampling cadence of the GMOS images is as small as 1 - 2 days, whereas the majority of photometric measurements for J004703.27–

204708.4 summarized in Table 2 of Solovyeva et al. (2020) have a typical cadence of months or years. Does the GMOS photometry of this star show signs of variability?

The light curve of J004703.27–204708.4 extracted from the GMOS observations is shown in Figure 7. The g' magnitudes obtained from GMOS are a few tenths of a magnitude brighter than might be expected based on the V magnitudes presented in Table 2 of Solovyeva et al. (2020). This could occur if the star was at a persistently bright phase of its light variations in mid to late 2008. The overall light level in the GMOS photometry may also be boosted by blending in the area immediately surrounding the star. Figure 6 of Solovyeva et al. (2020) shows that there are at least three moderately bright stars within a few tenths of an arcsec of the dominant source. To reduce possible contamination from nearby stars, Solovyeva et al. (2020) restricted their photometric measurements to images with an angular resolution < 0.8 arcsec, whereas those used to construct Figure 7 have an image quality > 1 arcsec.

There is jitter in the light curve in Figure 7, with an overall amplitude of ~ 0.1 magnitudes. There is also a tendency for J004703.27–204708.4 to become fainter towards later epochs. While the jitter is smaller in amplitude than that in the Solovyeva et al. light curve, the trend in declining brightness suggests that the variations seen in their light curve may occur on time scales of a month or more. The 1σ scatter of other stars with this brightness that were not flagged as variables is $\pm 0.02 – 0.03$ mag, which is smaller than the scatter in Figure 7. J004702.18–204739.9 was not flagged as a variable star in Section 3 because the scatter does not meet the 5σ selection criterion used there. Still, signs of variability are present in Figure 7.

6.2. New Bright Blue Variables in NGC 247

Given the likelihood that as yet undiscovered variables lurk in the photometric measurements, we have examined the light curves of objects within the red dashed lines in Figure 5. After limiting the sample to those sources that fall within the main body of the galaxy to reduce contamination from foreground/background objects, and rejecting obvious background galaxies, we find that the light curves of most objects show only marginal scatter in the GMOS observations: if variability occurs in these objects then it must be on timescales that exceed the six months that was sampled with GMOS.

After rejecting objects that have non-stellar morphologies, and hence are unresolved blends, there are two sources that show obvious scatter in the GMOS observations, indicating changes in light levels over the course of a few days to a few months. The light curves of

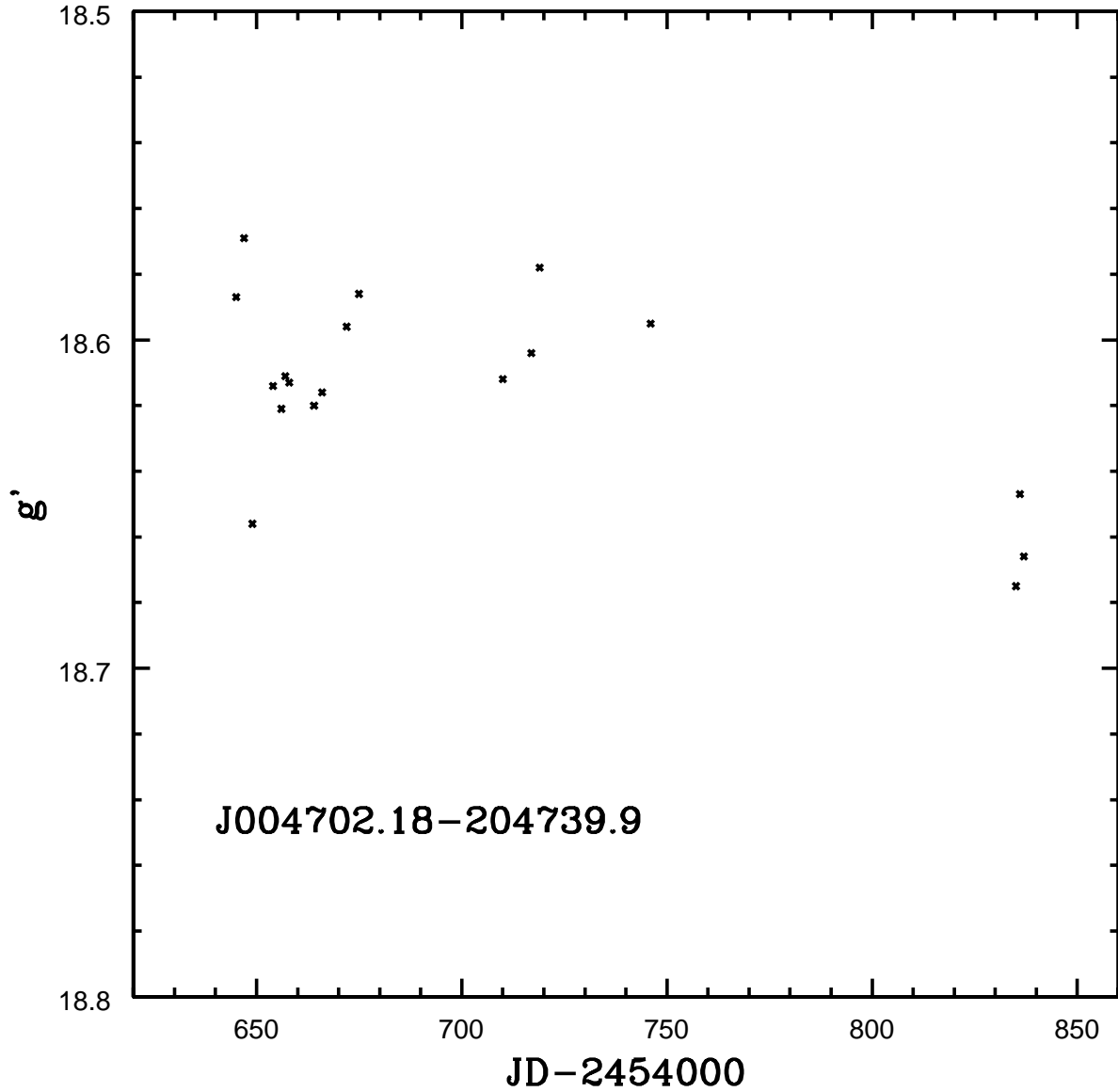


Fig. 7.— The g' light curve of J004702.18–204739.9, which Solovyeva et al. (2020) classify as a B[e] supergiant. Only measurements obtained from the GMOS images are shown. There is a ~ 0.1 magnitude throw in the GMOS measurements, and a hint of a long term decrease in mean brightness from mid 2008 to early 2009.

these stars are shown in Figure 8, where departures from mean light levels on a scale of many tenths of a magnitude are seen. Neither light curve shows signs of periodic behaviour. These objects would have been flagged as variables if a lower than 5σ dispersion criterion had been applied in Section 3.

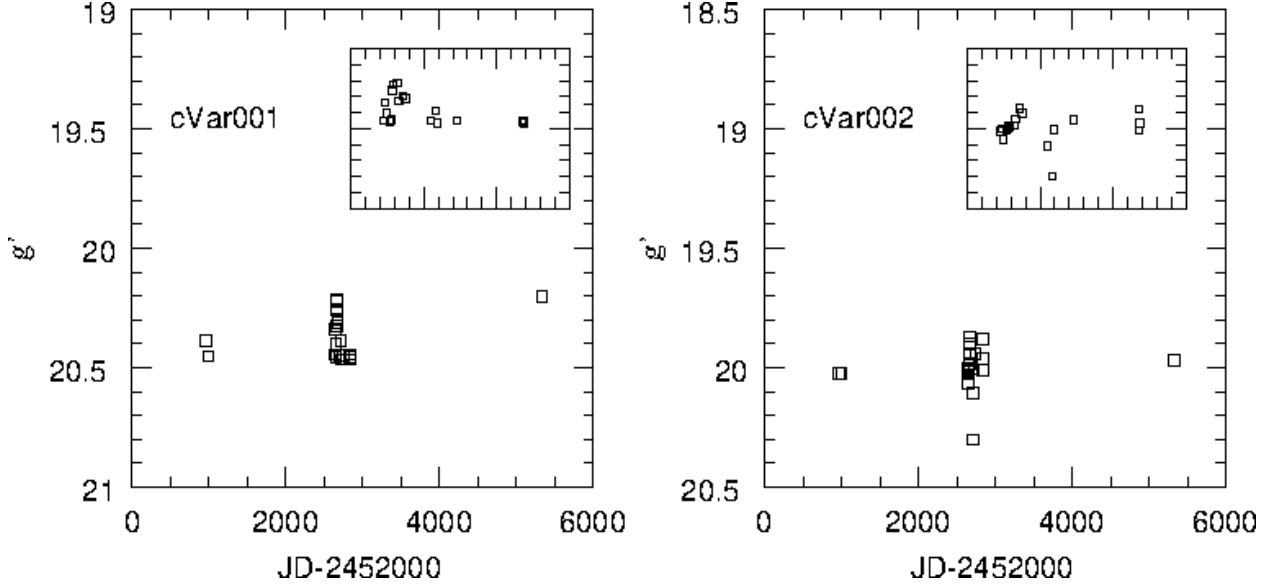


Fig. 8.— Light curves of luminous early-type variable stars in the disk of NGC 247 that were selected based on location in the CMD and are not obvious blends or background galaxies. The inset in each panel shows the GMOS data between JDs 2454600 and 2454900, with a 1 magnitude throw along the vertical axis.

The locations and photometric properties of these objects are listed in Table 5, while finding charts that cover 15×15 arcsec are shown in Figure 9. cVar001 is separated by ~ 2 arcsec from a star-forming complex, and it is possible that some of the variations in the light curve of this star may be affected by contamination from brighter nearby objects, especially in the images in the 1.5 arcsec FWHM grouping. Therefore, we consider the cVar001 light curve to be tentative. In contrast, cVar002 is relatively isolated, and so less prone to seeing-related variations in the light curve.

We have attempted to identify these objects in the SPITZER images examined by Davidge (2021). The SPITZER images have a poorer angular resolution than the GMOS observations, and cVar001 and the star-forming complex immediately to the south of it appear as a single object in the SPITZER data. Therefore, [3.6] and [4.5] measurements for this star are not given in Table 5. As for cVar002, it has [3.6]–[4.5] colors that do not depart from the primary sequence of objects in the ([3.6], [3.6] – [4.5]) CMD of NGC 247 shown in Davidge (2021), indicating that if emission from hot dust is present then it does

Name	RA (2000)	Dec (2000)	g'	$g'-r'$	$r'-i'$	[3.6]	[3.6]–[4.5]
cVar001	00:47:10.3	–20:48:53.9	20.437	-0.031	-0.416	–	–
cVar002	00:47:06.1	–20:46:45.1	20.007	0.041	0.016	17.23	0.09

Table 5: Blue Variables Identified from CMD Selection

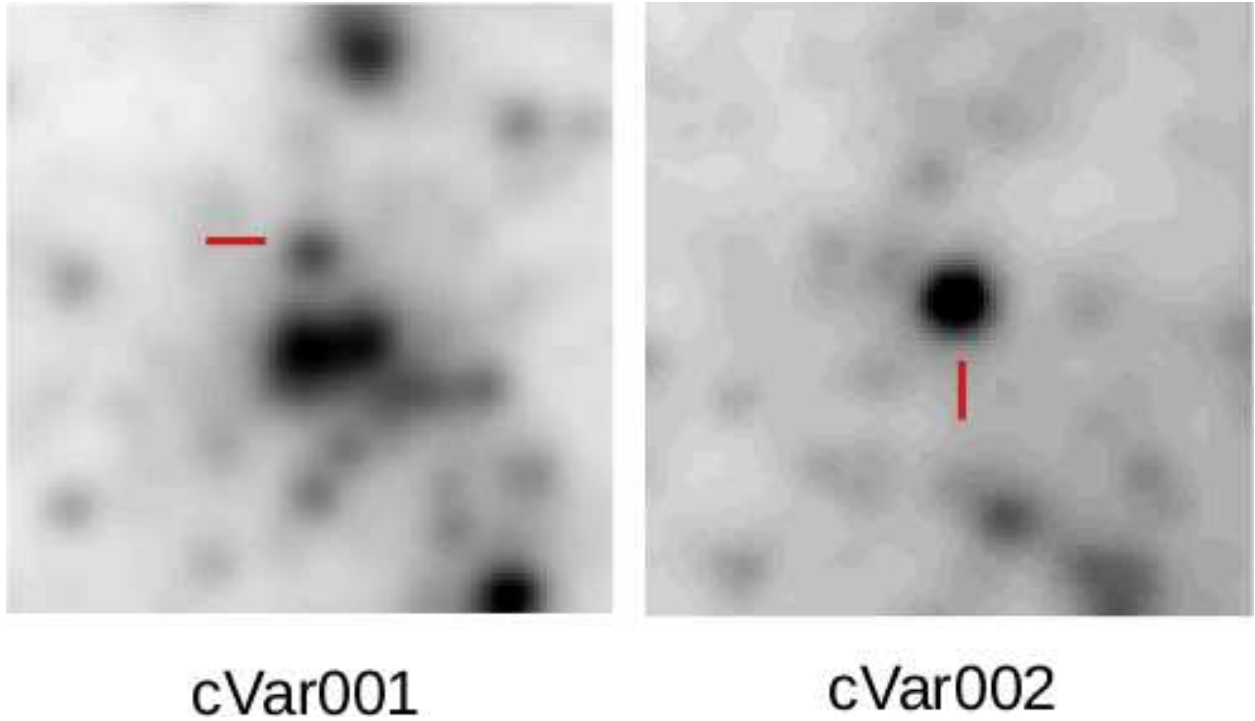


Fig. 9.— Same as Figure 1, but showing finding charts for the variables identified using a location on the CMD that corresponds to that of LBVs in the Galaxy and the Magellanic Clouds. Note that only cVar002 is isolated, as cVar001 is part of a star-forming complex.

not dominate over the photospheric light from the host object.

7. SUMMARY & DISCUSSION

Deep g' images obtained with GMOS on GS have been used to search for variable stars in the southern half of the nearby disk galaxy NGC 247. This part of NGC 247 contains areas of on-going and recent (i.e. within a few hundred Myr) star formation (Rodriguez et al. 2019; Davidge 2021), and so can be expected to harbor a rich population of luminous variable

stars that span a range of types. The GMOS observations cover a 7 month time period, with intensive coverage over a one month period. These observations are thus sensitive to periodic changes in light levels on time scales of a few days to tens of days. A mix of periodic and non-periodic variables are identified.

The time coverage has been extended using archival observations from the CFHT Mega-Cam and NOIRLab DECam. An extended time baseline is of greatest interest for variables that may have erratic light variations, such as LBVs. Observations from the SPITZER IRAC are also examined to search for evidence of hot circumstellar dust. A summary of the main findings is as follows:

1) Of the fifteen new variables that have been discovered, three are Cepheids. These were identified based on the dispersion in the magnitude measurements made from the ten GMOS images that have ~ 1 arcsec FWHM image quality. The newly discovered Cepheids have periods that are near the low end of those already discovered in NGC 247. Two previously identified Cepheids were also recovered.

Four Cepheids that were discovered by Garcia-Valera et al. (2008) in the area observed with GMOS were not detected. One failed detection was because the Cepheid (cep013) is located close to the edge of the GMOS science field, and an inspection of the GMOS photometry of that object reveals light variations that are consistent with those of a Cepheid. The failure to detect the other Cepheids is likely due to the shorter time coverage of the GMOS data when compared with that employed by Garcia-Valera et al. (2008). A shorter time baseline makes the sampling of variability susceptible to stochastic effects.

In addition to serving as standard candles, Cepheids probe the SFH of the host galaxy during the past few hundred Myr. The progenitors of fundamental mode Cepheids with periods like those found in this study likely formed within the past 100 Myr (e.g. Bono et al. 2005). This is shorter than the ~ 0.6 Gyr disk crossing time that results for NGC 247 if a rotational velocity of ~ 100 km/sec at the optical diameter of 19.9 arc minutes (Carignan & Puche 1990) and a distance of 3 Mpc are adopted. Hence, Cepheids with periods like those found to date likely have not had enough time to mix throughout the NGC 247 disk. Still, Cepheids will acquire random motions from interactions with molecular clouds, and they might have attained random velocities of $\sim 20 - 30$ km/sec if they have reached the equilibrium velocity dispersion of a host disk with a 100 km/sec rotation velocity (e.g. Kregel et al. 2005). Cepheids in the NGC 247 disk might then be expected to move projected distances of only 2 – 3 kpc from their places of birth over 100 Myr. The present study has found Cepheids in the southern disk that have periods that are comparable to the shortest period Cepheids found in the northern disk. That Cepheids with 20 – 30 day periods are

seen over much of the NGC 247 disk overcomes at least in part the lop-sided distribution of the Cepheids found by Garcia-Valera et al. (2008).

2) Eight new variables with blue colors have been discovered. Six of these were identified solely on the dispersion in their magnitude measurements with no knowledge of their colors, while two more were identified by targeting the area of the CMD that contains LBVs and then applying relaxed conditions to identify variability. The two brightest variables identified at the time the MegaCam data were recorded using the first technique (Var001 and Var009) have photometric properties that place them close to the S Dor instability strip in the $(i', g' - i')$ CMD. Depending on the epoch of observation and the amplitude of light variations, some of the fainter blue variables discovered using this technique may prove to have brightnesses and colors that could position them in the LBV region of the CMD.

Two differing models have been proposed to explain the nature of LBVs. Humphreys & Davidson (1994) review the photometric characteristics of LBVs, and suggest that they are massive single stars, and can be sorted into two group. The first group consists of the most massive stars that do not evolve to the RSG stage due to large-scale mass loss. These stars show large amplitude photometric variations that may be tied to mass ejection. The second group is fainter than the first, and shows less dramatic light curve variations. The stars in that group are thought to be experiencing mass loss after evolution as a RSG.

Smith & Tombleson (2015) and Smith (2017) present an alternate interpretation, suggesting that LBVs are massive blue stragglers that are the product of binary evolution. This is based on the finding that LBVs appear to be more isolated than the Wolf-Rayet stars that are thought to be the end point of massive single star evolution (but see Humphreys et al. 2016). In addition, there is evidence for supernovae that appear to have originated from massive stars that did not shed large quantities of their mass prior to explosion, which challenges the classical notion of mass loss throttling the evolution of massive stars. While Figure 6 indicates that there is an association between the cLBVs and areas of star formation in NGC 247, Figures 1 and 9 suggest that the majority of the early-type variables found here are embedded in complex environments, in the sense that they have one or more nearby companions, although cVar002 is an exception.

Wofford et al. (2020) review the statistics of LBVs and cLBVs in nearby galaxies, and emphasize the importance of identifying LBVs in a range of galaxy environments. NGC 247 is a potentially important target in this regard as it is one of only four galaxies searched so far for LBVs at visible wavelengths that show obvious tidal features. Table 1 of Wofford et al. (2020) lists three galaxies that show evidence of tidal distortion at the present day: the SMC, NGC 55, and DDO 68. These galaxies have M_K s that are 1 – 2 magnitudes fainter

than NGC 247, and together they contain 3 LBVs and 6 cLBVs. The present survey of the southern half of NGC 247 has found a comparable number of intrinsically bright blue variables.

The presence of tidal features might affect the incidence and spatial distribution of LBVs and related objects within a galaxy. As more galaxies with tidal distortions are searched for LBVs then this might provide insights into – say – the role that tidally-induced turbulence in the ISM plays in defining the frequency of LBVs in a galaxy. Indeed, environments that foster the formation of the largest giant molecular clouds will likely also have the highest probability of forming the most massive stars (e.g. Jerabkova et al. 2018). In the context of the model in which LBVs are single massive stars then one might expect a correlation between the incidence of LBVs and the masses of molecular clouds. Finally, galaxies that show prominent signs of tidal interaction also tend to have high SFRs concentrated in their central regions (e.g. Pan et al. 2019), and so the specific frequency of LBVs might be higher there.

M82 is a nearby tidally distorted galaxy that is a prime target to search for LBVs given its high SFR, although the extinction towards the active star forming regions make studies at visible wavelengths problematic. Nevertheless, using radio observations as an indicator, Matilla et al. (2013) identify an object with an absolute magnitude consistent with that of an LBV in outburst, although the nature of this source remains enigmatic. Surveys at longer wavelengths may also have found cLBVs in a range of other galaxies. The SPIRITS survey (Kasliwal et al. 2017) has identified IR transients that are associated with star-forming galaxies. These so-called SPRITES have photometric properties that are reminiscent of LBVs in eruptive phases.

LBVs are very rare objects, and are but one type of variable identified among intrinsically bright blue stars. Thus, while we have identified candidate LBVs in this study, we anticipate that subsequent observations will reveal that many – if not all – of the objects so identified will be found not to be true LBVs. This being said, *bona fide* LBVs may be missed in the present survey given that these objects can experience extended periods of photometric dormancy (Humphreys & Davidson 1994).

The 1 arcsec FWHM angular resolution of the GMOS images coupled with the crowded nature of star forming regions also means that many of the blue variables may be blended with stars of comparable (i.e. within 1 – 2 magnitudes) brightness. An inspection of HST images taken as part of the ANGST survey (Dalcanton et al. 2009) reveal that Var001 is actually a tight knot of stars, although there is a dominant star in this asterism that is ~ 2 magnitudes brighter than its companions. In contrast, Var009 is an isolated object.

Establishing the nature of the brightest blue variables found here will require spectroscopy and additional photometry to characterize the absorption and emission lines in their spectra, and to better characterize the time scale and amplitude of light variations. A possible hint as to the nature of the intrinsically bright blue variables found here is that none appear to show excess emission in the $3 - 5\mu\text{m}$ wavelength region. Despite their location in the CMD close to the S Doradus instability strip, there is thus no evidence for hot circumstellar dust shells, as might form from metal-enriched material ejected throughout their evolution. Of course, dusty envelopes that do not dominate the emission in the $3 - 5\mu\text{m}$ wavelength region might still be present. A search for cooler dust emission at longer wavelengths where the contribution from photospheric light is suppressed awaits measurements with arcsec or better angular resolutions.

- 3) The original motivation for the GMOS observing program that serves as the basis for this paper was to search for EBs that contain massive stars on or near the main sequence. Assuming that massive main sequence stars have $M_V \sim -5$ to -6 then such EBs will have $g' \sim 22 - 23$ in NGC 247. While some of the blue variables found here have brightnesses in this range, their light curves do not show variations that are consistent with EBs. However, one of the blue variables that falls well below the S Dor instability strip on the $(i', g' - i')$ CMD shows periodic variations that are sinusoidal in nature. We speculate that these variations are the result of star-to-star interactions in a close binary system, with the variations presumably related to spot activity on one of the stars. If the period found here is off by a factor of two then the light curve would be that of an ellipsoidal variable. Radial velocity measurements of this object that cover many tens of days should reveal if it is part of a binary system and – if so – the true period of the variability.
- 4) Two cLBVs were found by targeting the region of the CMD that contains the intrinsically brightest LBVs (see above). The frequency of variability among stars in this part of the CMD may provide clues into the nature of these objects and the chances of their detection in surveys that are similar to this one. In fact, the time series photometric properties of the majority of intrinsically luminous blue stars in the main body of the galaxy showed little or no signs of variability from June 2008 to January 2009. The frequency of detection over this time frame was $\frac{2}{10} = 0.2$, with a threshold amplitude for variability detection ~ 0.1 magnitudes. The photometrically stable stars in this part of the CMD may simply have been observed during a quiet phase of their evolution. It is unlikely that the photometrically stable stars are in the foreground given that they are seen against in the main body of NGC 247 and are close to star forming regions. Obvious background galaxies were also deleted from the sample.

5) The photometric variability of the spectroscopically classified B[e] star J004702.18–204739.9, which is one of the brightest stars in NGC 247, has been examined with the GMOS images. These data have a sampling cadence that is finer than measurements used by Solovyeva et al. (2020) to examine the photometric stability of this star. Non-periodic variations of a few hundredths of a magnitude over timescales of a few days are found, with a ~ 0.1 magnitude systematic decrease in g' over a six month time span. J004702.18–204739.9 is in a crowded environment and is likely blended with other objects in the GMOS images. Thus, the intrinsic variations in the dominant star in the blended conglomeration are probably larger than those seen here.

6) Four semi-regular variables have also been identified. Three of these have red colors, and are classified as type SRb. These are located in or near dense stellar knots and associations, which is consistent with them being young, highly evolved objects. These stars have intrinsic brightnesses that are similar to those of the classic Galactic semi-regular variable Betelgeuse (α Ori).

The fourth semi-regular variable has a $g'–i'$ color that is indicative of an intermediate spectral-type, and a light curve that shows variations that are reminiscent of those associated with RCrB stars. It has been classified as type SRd in this study. Longer term photometric monitoring of this star will be useful to determine if it shows the persistent moderately long-term deep dips in its brightness that are the defining photometric characteristic of RCrB stars. RCrB stars are rare, and may be the result of a merger of white dwarfs (e.g. Tisserand et al. 2020), making them of inherent interest for probing the most advanced and exotic stages of binary star evolution. To the best of our knowledge, this is the first candidate RCrB star to be identified outside of the Local Group. A survey for stars of this type among nearby galaxies will provide statistics that will help identify the nature of these objects.

Surveys for variable stars in NGC 247 have so far explored only the tip of the iceberg, and there is much room for future exploration. The detection of variable stars with smaller amplitudes than those found here and/or of fainter sources will require deeper time series photometry with sub-arcsecond angular resolutions. Such observations would enable a search for fainter Cepheids with shorter periods than those found to date in NGC 247. The Cepheids found in such a survey could be used to examine the spatial extent of star formation in NGC 247 a few hundred Myr in the past, which is an epoch when there is evidence for large-scale star formation in at least some parts of the galaxy. High angular resolution observations will also enable the exploration of intrinsically crowded environments, such as the dense star forming complexes where LBVs might be present.

While massive stars in binary systems are likely the norm (e.g. Sana et al. 2012), the

detection of massive EBs in NGC 247 has so far remained elusive. However, the detection and characterization of even one or two of these will provide a fundamental constraint on the distance to NGC 247 that is based on purely geometric arguments. While challenging, obtaining the precise radial velocity curves for massive EBs in NGC 247 and other galaxies with similar distances that are required for such a project should be possible with the upcoming generation of 30 - 40 meter telescopes.

It is a pleasure to thank the anonymous referee for a timely report and thoughtful comments that greatly improved the manuscript.

REFERENCES

Allen, C. W., *Astrophysical Quantities*, Fourth Edition, A. N. Cox, editor (Athlone: London)

Almeida, L. A., Sana, H., de Mink, S. E., et al. 2015, *ApJ*, 812, 102

Bono, G., Marconi, M., Cassisi, S., Caputo, F., Gieren, W., & Pietrzynski, G. 2005, *ApJ*, 621, 966

Boulade, O., Charlot, X., Annon, P., et al. 2003, *Proc. SPIE*, 4841, 72

Carignan, C. 1985, *ApJS*, 58, 107

Carignan, C., & Puche, D. 1990, *AJ*, 100, 641

Clayton, G. C. 1996, *PASP*, 108, 225

Di Criscienzo, M., Marconi, M., Musella, I., Cignoni, M., & Ripepi, V. 2013, *MNRAS*, 428, 212

Dalcanton, J. J., Williams, B. F., Seth, A. C., et al. 2009, *ApJS*, 183, 67

Davidge, T. J. 1988, *AJ*, 95, 731

Davidge, T. J. 2006, *ApJ*, 641, 822

Davidge, T. J. 2021, *AJ*, 161, 93

de Jager, C., & Nieuwenhuijzen, H. 1987, *A&A*, 177, 217

Fazio, G. G., Hora, J. L., Allen, L. E., et al. 2004, *ApJS*, 154, 10

Flaugher, B., Diehl, H. T., Honscheid, K., et al. 2015, *AJ*, 150, 150

Ferguson, A. M. N., Wyse, R. F. G., Gallagher III, J. S., & Hunter, D. A. 1996, *AJ*, 111, 2265

Fukugita, M., Ichikawa, T., Gunn, J. E., Doi, M., Shimasaku, K., & Schneider, D. P. 1996, AJ, 111, 1748

Garcia-Varela, A., Pietrzynski, G., Gieren, W., et al. 2008, AJ, 136, 1770

Gieren, W., Pietrzynski, G., Bresolin, F., et al. 2005, Msngr, 121, 23

Gieren, W., Pietrzynski, G., Soszynski, I., et al. 2009, ApJ, 700, 1141

Hook, I., Jorgensen, I., Allington-Smith, J. R., Davies, R. L., Metcalfe, N., Murowinski, R. G., & Crampton, D. 2004, PASP, 116, 425

Howard, C. S., Pudritz, R. E., Sills, A., & Harris, W. E. 2019, MNRAS, 486, 1146

Hubble, E. 1925, ApJ, 62, 409

Humphreys, R. M., & Davidson, K. 1994, PASP, 106, 1025

Humphreys, R. M., Weis, K., Davidson, K., & Gordon, M. S. 1016, ApJ, 825, 64

Humphreys, R. M., Gordon, M. S., Martin, J. C., Weis, K., & Hahn, D. 2017, ApJ, 836, 64

Humphreys, R. M., Stangl, S., Gordon, M. S., Davidson, K., & Grammer, S. H. 2019, AJ, 157, 22

Jarrett, T. H., Chester, T., Cutri, R., Schneider, S. E., Huchra, J. P. 2003, AJ, 125, 525

Jerabkova, T., Hasani Zonoozi, A., Kroupa, P., Beccari, G., Yan, Z., Vazdekis, A., & Zhang, Z-Y 2018, A&A, 620, A39

Kacharov, N., Neumayer, N., Seth, A. C., Cappellari, M., McDermid, R., Walcher, C. J., & Böker, T. 2018, MNRAS, 480, 1973

Karachentsev, I. D., Grebel, E. K., Sharina, M. E. 2003, A&A, 404, 93

Kasliwal, M. M., Bally, J., Masci, F., et al. 2017, ApJ, 839, 88

Kregel, M., van der Kruit, P. C., & Freeman, K. C. 2005, MNRAS, 358, 503

Lambert, D. L., Rao, N. K., Pandey, G., Ivans, I. I. 2001, ApJ, 555, 925

Magnier, E. A., & Cuillandre, J.-C. 2004, PASP, 116, 449

Martin, J. C., & Humphreys, R. M. 2017, AJ, 154, 81

Massey, P., McNeill, R. T., Olsen, K. A. G., et al. 2007, AJ, 134, 2474

Mattila, S., Fraser, M., Smartt, S. J. et al. 2013, MNRAS, 431, 2050

Pan, H-A, Lin, L., Hsieh, B-C, et al. 2019, ApJ, 881, 119

Prieto, J. L., Stanek, K. Z., Kochanek, C. S., et al. 2008, ApJ, 673, L59

Rodriguez, M. J., Baume, G., & Feinstein, C. 2019, A&A, 626, A35

Russell, H. N. 1912a, *ApJ*, 35, 319

Russell, H. N. 1912b, *ApJ*, 36, 54

Sana, H., de Mink, S. E., de Koter, A. et al. 2012, *Sci*, 337, 444

Smith, N., Vink, J. S., & de Koter, A. 2004, *ApJ*, 615, 475

Smith, N. 2014, *ARA&A*, 52, 487

Smith, N., & Tombleson, R. 2015, *MNRAS*, 447, 598

Smith, N. 2017, *Phil. Trans. R. Soc.*, A375, 20160268

Smith N., Aghakanloo, M., Murphy, J. W., Drout, M. R., Stassun, K. G., Groh, J. H. 2019, *MNRAS*, 488, 1760

Solovyeva, Y., Vinokurov, A., Sarkisyan, A., et al. 2020, *MNRAS*, 497, 4834

Stetson, P. B. 1987, *PASP*, 99, 191

Stetson, P. B. 1994, *PASP*, 106, 250

Storm, J., Gieren, W., Fouque, P., et al. 2011, *A&A*, 534, A94

Tisserand, P., Clayton, G. C., Bessell, M. S. et al. 2020, *A&A*, 635, A14

Toribio San Cipriano, L., Dominguez-Guzman, G., Esteban, C., et al. 2017, *MNRAS*, 467, 3759

Webbink, R. F. 1976, *ApJ*, 209, 829

Werner, M. W., Roellig, T. L., Low, F. J., et al. 2004, *ApJS*, 154, 1

Wofford, A., Ramirez, V., Lee, J. C., et al. 2020, *MNRAS*, 493, 2410